Biochemical and Biophysical Research Communications 383 (2009) 83–87

Contents lists available at ScienceDirect

Biochemical and Biophysical Research Communications

journal homepage: www.elsevier.com/locate/ybbrc

Snapshot of a Michaelis complex in a sulfuryl transfer reaction: Crystal structure of a mouse sulfotransferase, mSULT1D1, complexed with donor substrate and accepter substrate

Takamasa Teramoto [a], Yoichi Sakakibara [b], Ming-Cheh Liu [c], Masahito Suiko [b], Makoto Kimura [a,d], Yoshimitsu Kakuta [a,d,*]

[a] Laboratory of Structural Biology, Department of Systems Life Sciences, Graduate School, Faculty of Agriculture, Kyushu University, Hakozaki 6-10-1, Higashi-ku, Fukuoka 812-8581, Japan
[b] Laboratory of Applied Biochemistry, Department of Biochemistry and Applied Biosciences, Faculty of Agriculture, University of Miyazaki, Miyazaki 889-2192, Japan
[c] Department of Pharmacology, College of Pharmacy, The University of Toledo, Toledo, OH 43606, USA
[d] Laboratory of Biochemistry, Department of Bioscience and Biotechnology, Graduate School, Faculty of Agriculture, Kyushu University, Hakozaki 6-10-1, Higashi-ku, Fukuoka 812-8581, Japan

ARTICLE INFO

Article history:
Received 9 March 2009
Available online 1 April 2009

Keywords:
Crystal structure
Sulfotransferase
Michaelis complex
Sulfuryl transfer reaction

ABSTRACT

We report the crystal structure of mouse sulfotransferase, mSULT1D1, complexed with donor substrate 3′-phosphoadenosine 5′-phosphosulfate and accepter substrate *p*-nitrophenol. The structure is the first report of the native Michaelis complex of sulfotransferase. In the structure, three proposed catalytic residues (Lys48, Lys106, and His108) were in proper positions for engaging in the sulfuryl transfer reaction. The data strongly support that the sulfuryl transfer reaction proceeds through an S_N2-like in-line displacement mechanism.

Introduction

Sulfonation is a widespread biological sulfuryl transfer reaction catalyzed by members of a family of enzymes, called cytosolic sulfotransferases (SULTs) [1]. SULTs utilize 3′-phosphoadenosine 5′-phosphosulfate (PAPS) as the sulfonate donor to catalyze the sulfonation of various substrate compounds, yielding 3′-phosphoadenosine 5′-phosphate (PAP) and sulfonate conjugates [1]. It has been reported that SULTs may also catalyze the reverse reaction (Fig. 1) [2]. These enzymes are involved in the Phase II detoxification of xenobiotics as well as in the homeostasis of catecholamine neurotransmitters and steroid/thyroid hormones, as well as cholesterol and its metabolites [3,4]. SULTs have recently become a focus of intense research with regard to their roles in cancer, drug metabolism, and pharmacogenetics [5,6].

Mouse SULT1D1 (mSULT1D1) has recently been shown to exhibit sulfonating activities toward catecholamines [7] and play a significant role in the metabolism of a broad range of xenobiotics [8]. We have been studying the structure and function of mSULT1D1 [8–10]. By solving the crystal structure of mSULT1D1 at a high resolution, we demonstrated that a water molecule, through interactions with Ile148 and Glu247 of the main chain, is critical to the recognition of dopamine by mSULT1D1 [9], and these two key amino acid residues (Ile148 and Glu247) may undergo conformational changes upon binding with different substrate, thereby allowing mSULT1D1 to recognize a variety of accepter substrate compounds [10].

To date, a number of structural and functional studies designed to clarify the reaction mechanisms of SULTs has been reported [11–13]. In particular, SULT1E1 is the most thoroughly studied SULT with respect to the sulfuryl transfer mechanism. This is mainly because that the crystal structures have been determined for mouse SULT1E1 (mSULT1E1) complexed with PAP/estrogen (E_2 (PDB Code: 1AQU) [14] or PAP/vanadate (1BO6) [15]; human SULT1E1 (hSULT1E1) complexed with PAPS (1HY3) [16]. These structures have helped us to project a ternary complex of the SULT with donor and acceptor substrates, i.e., the Michaelis complex, and this information, in turn, has been used to design the mutational analysis [15], kinetic isotope effect experiments [17] and the calculation of reaction pathway by QM/MM method [18] to gain insight into

* Corresponding author. Address: Laboratory of Biochemistry, Department of Bioscience and Biotechnology, Graduate School, Faculty of Agriculture, Kyushu University, Hakozaki 6-10-1, Higashi-ku, Fukuoka 812-8581, Japan. Fax: +81 92 642 2854.
E-mail address: kakuta@agr.kyushu-u.ac.jp (Y. Kakuta).

0006-291X/$ - see front matter © 2009 Elsevier Inc. All rights reserved.
doi:10.1016/j.bbrc.2009.03.146

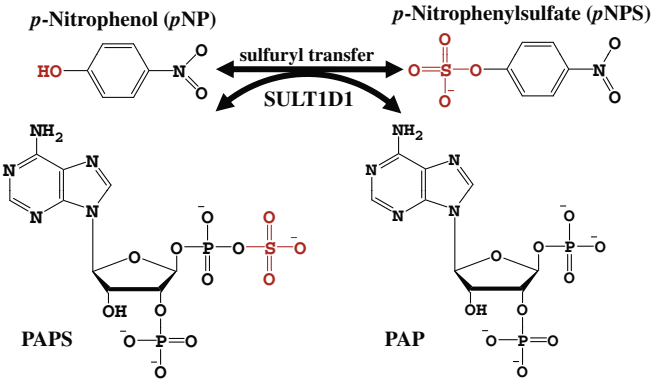

Fig. 1. The scheme of sulfuryl transfer reaction catalyzed by mSULT1D1. *p*-Nitrophenol (*p*NP) is illustrated as a model acceptor substrate.

the sulfuryl transfer mechanism. These studies have resulted in the identification of three crucial active site residues, Lys48, Lys106, and His108, and led to the proposal of a concerted, in-line sulfuryl transfer mechanism. The presumed Michaelis complex thus has furnished a considerable amount of information concerning the sulfuryl transfer reaction mediated by SULT. In spite of the information that has been generated, however, no crystal structure of a Michaelis complex of SULT has been reported.

We report here the structures of four distinct mSULT1D1 crystals prepared using co-crystallization and soaking method. The crystal structures determined were those of mSULT1D1 complexed with PAPS alone, PAPS plus *p*NPS, PAPS plus *p*NP, and PAP plus *p*NP. Among them, the mSULT1D1–PAPS–*p*NP complex represented the first crystal structure of a Michaelis complex of the SULT family which illustrates the reactive state prior to the sulfuryl transfer reaction. Our data on the structure of the Michaelis complex are consistent with those previously reported in the structural and functional studies on the reaction mechanisms of members of the SULT family.

Materials and methods

Preparation of four distinct mSULT1D1 crystals. Procedures for the expression, purification, and crystallization of recombinant mSULT1D1 have previously been reported [8–10].

mSULT1D1–PAPS complex. Crystallization was carried out using the hanging drop vapor diffusion method. The protein solution contained 8 mg/ml of purified mSULT1D1, 50 mM Tris–HCl, pH 7.9, 150 mM NaCl, 10 mM dithiothreitol (DTT), and 5 mM PAPS. After mixing protein and reservoir solutions (16% PEG 10,000, 10 mM DTT, and 100 mM Bis–Tris, pH 5.5) in a 1:1 ratio, crystals were grown following a 3-day incubation at 20 °C.

mSULT1D1–PAPS–pNPS complex. The mSULT1D1–PAP crystals were soaked into a solution containing 50 mM Tris–HCl (pH 7.9), 150 mM NaCl, 10 mM DTT, 5 mM PAP, 16% PEG 10,000, 100 mM Bis–Tris (pH 5.5), 25% glycerol, and 100 mM *p*NPS for 30 s.

mSULT1D1–PAPS (PAP)–pNP complex and mSULT1D1–PAP–pNP complex. The mSULT1D1–PAPS–*p*NPS crystals were soaked into a solution containing 50 mM Tris–HCl (pH 7.9), 150 mM NaCl, 10 mM DTT, 5 mM PAP, 16% PEG 10,000, 100 mM Bis–Tris (pH 5.5), 25% glycerol, and saturating *p*NP for 30 s (for mSULT1D1–PAPS (PAP)–*p*NP complex) and for 90 s (for mSULT1D1–PAP–*p*NP complex).

The crystals prepared as described above were individually mounted on a cryo-loop, and flash-cooled with a nitrogen gas stream at 100 K using a cryosystem (Rigaku).

Data collection, structure determination, and refinement. X-ray diffraction data were collected with Jupiter210 CCD (Rigaku/MSC) and synchrotron radiation at beamline BL38B1 of SPring-8. All diffraction data were processed using the program package HKL2000 [19]. All crystals were found to belong to the space group *C*2. Data collection statistics are summarized in Table 1.

The crystal structures of mSULT1D1 complexes were determined by molecular replacement using Molrep [20]. The previously reported mSULT1D1 structure (Protein Data Bank Accession Entry 1ZPT) [9] was used as a searching model. All refinements of data were carried out using refmac5 [21]. Iterative cycles of refinements and manual rebuilding in Coot [22] were carried out until the free *R*-factor converged. Stereochemical checks were performed using PROCHECK [23]. Refinement statistics are summarized in Table 1.

The atomic coordinates and structure factors of mSULT1D1–PAPS complex, mSULT1D1–PAPS–*p*NPS complex, mSULT1D1–PAPS (PAP)–*p*NP complex, and mSULT1D1–PAP–*p*NP complex have been deposited in the Protein Data Bank at Rutgers University under Accession Codes 2ZYT, 2ZYU, 2ZYV, and 2ZYW, respectively.

Results and discussion

Crystal structure of the mSULT1D1–PAPS complex

The mSULT1D1 crystal complexed with PAPS diffracted up to 1.55 Å and a clear electron density of PAPS was observed (Fig. 2C). In the structure, the SO_3 moiety of PAPS formed interaction with a few amino acid residues and waters. One oxygen of the SO_3 moiety was coordinated to the side chain of Lys48 (3.2 Å). Another oxygen was in position to form interaction with the side chain of Lys106 (3.2 Å) and a water molecule (3.2 Å) which interacted also with the side chain of Thr52, Lys106, and Tyr240. The third oxygen was in position to form interaction with the side chain nitrogen (Nε2) of His108 (3.0 Å) and the backbone amide of Lys48 (2.9 Å). The side chains of Lys106 and His108 were coordinated to a well-ordered water molecule which corresponded to an acceptor phenolic hydroxyl group of *p*NP when the mSULT1D1–PAPS structure was superimposed with the mSULT1D1–PAP–*p*NP structure [10].

Compared with the hSULT1E1–PAPS structure (PDB Code: 1HY3) which is the only PAPS-bound SULT structure solved to date [16], the amino group of the side chain of the catalytic Lys48 adopted a different orientation in the mSULT1D1–PAPS structure. In the hSULT1E1–PAPS structure, the side chain nitrogen of the catalytic Lys47 (which corresponds to Lys48 in mSULT1D1) formed interaction with the side chain hydroxyl of Ser137 (which corresponds to Ser138 in mSULT1D1). Whereas in the mSULT1D1–PAPS structure, the side chain of the catalytic Lys48 formed interaction with the bridging oxygen (2.9 Å) between the 5′-phosphate and sulfonate groups of the PAPS molecule as is seen in the PAP-bound structures [9]. The structural difference of the catalytic Lys residue between mSULT1D1 and hSULT1E1 suggested that the residue may be able to adopt two different conformations in PAPS-complexed structure.

Crystal structure of the mSULT1D1–PAPS–pNPS complex

We first attempted to prepare a mSULT1D1–PAP–*p*NPS complex (the enzyme–product (EP) complex) by soaking mSULT1D1–PAP crystal (Fig. 2A) in 100 mM *p*NPS solution for 30 s. Afterwards, the crystal was mounted on a cryo-loop, and flash-cooled with a nitrogen gas stream at 100 K. Unexpectedly, mSULT1D1 crystal complexed with PAPS and *p*NPS was obtained due to the reverse reaction catalyzed by mSULT1D1 (Fig. 1). The reverse reaction catalyzed by SULT had previously been reported in the enzymatic assay of hSULT1E1 [2]. In the reverse reaction, the sulfonate group was transferred from *p*NPS to PAP under the action of mSULT1D1, resulting in the formation of PAPS and *p*NP in the crystal. More-

Table 1
Data collection and refinement statistics.

Data collection	PAPS	PAPS–*p*NPS	PAPS (PAP)–*p*NP	PAP–*p*NP
Space group	*C*2	*C*2	*C*2	*C*2
Unit cell parameters	a = 160.2 Å	a = 152.9 Å	a = 155.2 Å	a = 155.3 Å
	b = 65.2 Å	b = 66.6 Å	b = 67.8 Å	b = 67.8 Å
	c = 46.8 Å	c = 42.6 Å	c = 42.9 Å	c = 42.9 Å
	$\alpha = \gamma$ = 90.0°	$\alpha = \gamma$ = 90.0°	$\alpha = \gamma$ = 90.0°	$\alpha = \gamma$ = 90.0°
	β = 104.2°	β = 106.1°	β = 105.2°	β = 105.3°
Beam line		SPring-8 BL38B1		
Wavelength (Å)	1.0000	1.0000	1.0000	1.0000
Resolution range (Å)	50.0–1.55	50.0–1.70	50.0–1.81	50.0–1.80
No. of reflections				
Observed/unique	177,072/55,335	128,209/44,210	139,140/38,650	143,074/39,743
Redundancy	3.2 (2.5)	2.9 (2.5)	3.6 (3.3)	3.6 (3.4)
R_{sym} [a,b]	0.093 (0.527)	0.0043 (0.817)	0.044 (0.404)	0.044 (0.387)
$I/\sigma(I)$ [a]	14.2 (1.2)	27.5 (1.1)	24.2 (1.9)	23.9 (2.1)
Completeness (%)	81.4 (42.8)	95.7 (93.7)	98.4 (94.7)	99.7 (99.3)
Refinement statistics				
Resolution range (Å)	34.67–1.55	24.66–1.80	21.45–1.81	26.17–1.80
No. of reflections				
Working set/test set	52,526/2782	34,757/1865	36,700/1940	37,750/1990
Completeness (%)	81.3	96.2	98.1	99.7
R_{cryst} [c] (%)/R_{free} [d] (%)	19.1/21.0	19.3/22.4	17.9/20.3	18.2/19.5
Root mean square deviations				
Bond length (Å)	0.008	0.011	0.010	0.007
Bond angles (°)	1.2	1.4	1.3	1.2
Average *B*-factor (Å2)/No. of atoms				
Protein	22.1/2510	26.7/2451	24.4/2468	23.2/2452
PAPS	19.7/31	24.4/31		
PAP moiety			20.0/27 [1.0] [e]	
SO_3 moiety			22.1/4 [0.4] [e]	
PAP				18.0/27
*p*NPS		48.8/14		
*p*NP[1]			29.9/10	24.3/10
*p*NP[2]			39.2/10	30.1/10
Glycerol	52.8/12	54.6/12	47.2/36	42.4/18
Water	30.8/229	34.2/173	35.8/223	33.6/226
Ramachandran analysis				
Most favored (%)	92.8	92.7	93.1	92.0
Allowed (%)	7.2	7.3	6.9	8.0
Generously allowed (%)	0.0	0.0	0.0	0.0
Disallowed (%)	0.0	0.0	0.0	0.0

[a] Values in parentheses are for the highest-resolution shell.
[b] $R_{sym} = \Sigma(I - \langle I\rangle)/\Sigma\langle I\rangle$, where I is the intensity measurement for a given refraction and $\langle I\rangle$ is the average intensity for multiple measurements of this refraction.
[c] $R_{cryst} = \Sigma||F_{obs}| - |F_{cal}||\ \Sigma F_{obs}$, where F_{obs} and F_{cal} are observed and calculated structure factor amplitudes.
[d] R_{free} value was calculated for R_{cryst}, using only an unrefined randomly chosen subset of reflection data (5%).
[e] Values in [ ] are for the occupancies.

over, the *p*NP molecule appeared to have quickly diffused out into the solution and the *p*NPS was simultaneously bound, since the soaking solution contained a relatively high concentration (100 mM) of *p*NPS. Therefore, both PAPS and *p*NPS were observed in the crystal structure (Fig. 2B).

Superposition of the mSULT1D1–PAPS–*p*NPS structure with the mSULT1D1–PAPS structure revealed the rmsd value of 0.19 Å for 264 Cαs. Overall, the two structures were virtually identical. The binding mode of PAPS to the active site in the mSULT1D1–PAPS–*p*NPS structure was also identical to that in the mSULT1D1–PAPS structure. The side chain of the catalytic Lys48 in mSULT1D1–PAPS–*p*NPS also formed interaction with the bridging oxygen (3.0 Å).

In mSULT1D1–PAPS–*p*NPS complex, *p*NPS was bound in a nonproductive manner and formed no interactions with the catalytic residues. The SO_3 moiety of *p*NPS formed interactions with two water molecules. One oxygen of the SO_3 moiety formed interaction with a water molecule which was strongly involved in recognition of dopamine in the previously reported model of mSULT1D1–dopamine complex [9], and another oxygen formed interaction with a different water molecule. The phenolic ring of *p*NPS formed hydrophobic interactions with the side chains of Leu84, Met243, and Met248, and the nitro group formed interactions with Glu247 and a water molecule. The structure in which the *p*NPS is bound in a nonproductive manner implies *p*NPS may inhibit reverse reaction (substrate inhibition) at high concentrations.

Crystal structure of the mSULT1D1–PAPS (PAP)–pNP complex

Because reproducibility of co-crystallization with PAPS for obtaining the PAPS-bound mSULT1D1 crystal was very low, mSULT1D1–PAPS–*p*NPS crystals were used in following experiments. The mSULT1D1–PAPS–*p*NPS crystal was soaked in the *p*NP-saturated solution for 30 s. Afterwards, the crystal was mounted on a cryo-loop, and flash-cooled with a nitrogen gas stream at 100 K. Clear electron densities of both PAPS and *p*NP were observed at 1.8 Å resolution (Fig. 2D). The complex structure revealed the presence of two *p*NP molecules (designated *p*NP[1] and *p*NP[2]) in accepter substrate binding pocket (Fig. 2D). The binding manner of the two *p*NP molecules was identical to that in previously reported mSULT1D1–PAP–*p*NP structure [10]. During refinement, we noticed the crystal was the mixture of

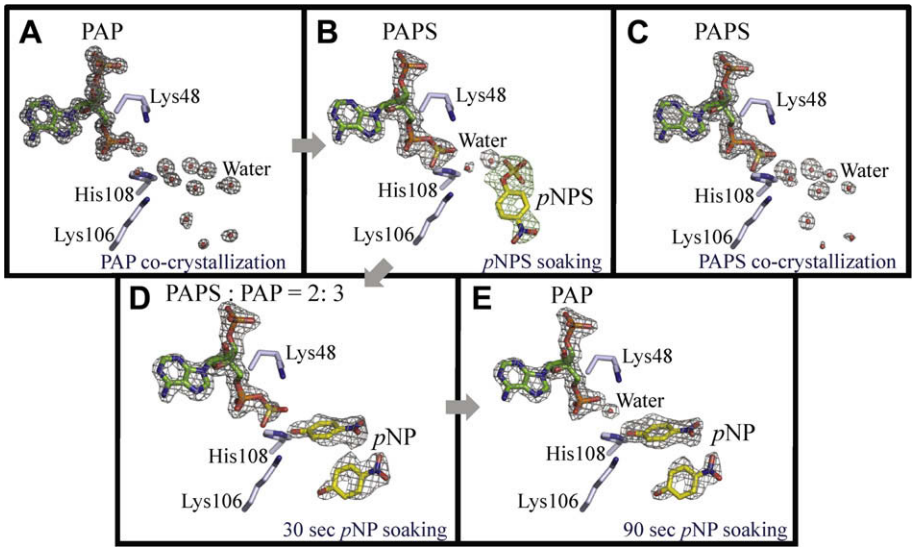

Fig. 2. Active site structures of mSULT1D1 complexed with (A) PAP alone, (B) PAPS plus *p*NPS, (C) PAPS alone, (D) PAPS plus *p*NP and PAP plus *p*NP, and (E) PAP plus *p*NP. The three key residues are shown in a stick model. The electron density maps in the active site are shown. The gray and green omit F_o–F_c maps were contoured at 5 σ and 3 σ, respectively. (For interpretation of the references to color in this figure legend, the reader is referred to the web version of this paper.)

mSULT1D1–PAPS–*p*NP structure and mSULT1D1–PAP–*p*NP structure. To estimate the occupancies of PAPS, PAP, and *p*NP in the crystal, we tried refinement with possible occupancies of them (Supplementary Table). Based on the results, it was estimated that the occupancy of the sulfonate group of PAPS was 0.4, indicating that PAPS and PAP were present at a ratio of two to three in the crystal. In contrast, the occupancy of the *p*NP[1] was estimated to be around 1. In addition, no multiple conformations of residues were observed in the active site. These results therefore revealed that the ratio of the mSULT1D1–PAPS–*p*NP complex and the mSULT1D1–PAP–*p*NP complex was two to three in the crystal and these two structures were virtually identical except for the sulfonate group of PAPS. The structure in which mSULT1D1 complexed with PAPS and *p*NP may indeed represented an 'enzyme–substrate complex' (ES-complex), i.e., the Michaelis complex. In the mSULT1D1–PAPS–*p*NP complex, *p*NP[1] was bound in a catalytically competent manner, and the acceptor phenolic hydroxyl group formed hydrogen bonds with the side chains of catalytic residues His108 (2.5 Å) and Lys106 (2.9 Å), located closely to the sulfonate group of PAPS with the hydroxyl group of *p*NP being approximately 3.1 Å away from the sulfur atom of PAPS.

Crystal structure of the mSULT1D1–PAP–pNP complex

Upon a 90-s soaking of the mSULT1D1–PAPS–*p*NPS crystal in a solution containing saturating *p*NP, electron densities of PAP and *p*NP were clearly observed (Fig. 2E). The occupancies of PAP and the two *p*NP molecules were estimated to be 1 by refinement process. Compared with the mSULT1D1–PAPS (PAP)–*p*NP structure, the electron density of SO_3 moiety of PAPS was not observed in the active site and, instead, a water molecule was bound at the same location. These could be shown in the clear positive electron density of sulfate moiety in the F_o (30 s *p*NP soak)-F_o (90 s *p*NP soak) map (Supplementary Figure). Therefore, the phenolic hydroxyl group of *p*NP[1] appeared to form hydrogen bonds with the water molecule (2.7 Å), which was also found in the previously reported mSULT1D1–PAP–*p*NP structure [10]. The electron density data obtained for mSULT1D1–PAPS–*p*NPS crystal soaking for 30 s and that soaking for 90 s in *p*NP-saturated solution revealed the sulfuryl group transfer from PAPS to *p*NP and the diffusion of the product, *p*NPS, out into the solution and the concomitant replacement with *p*NP. Upon soaking for 30 s, a reduction in the occupancy of SO_3 moiety of PAPS was observed in the mSULT1D1–PAPS(PAP)–*p*NP structure, which could be attributed to the transfer reaction catalyzed by mSULT1D1 using the some 60% of bound PAPS in the crystal. Upon soaking for 90 s, the PAPS originally present was completely converted to PAP under the action of mSULT1D1.

Michaelis complex of the mSULT1D1-catalyzed sulfuryl transfer reaction

The above-mentioned results indicate that the mSULT1D1–PAPS–*p*NP complex structure may in fact represent an active Michaelis complex that is ready to engage in the forward reaction. We have thus determined the bona fide Michaelis complex without the use of mutants of catalytic residues and/or nonreactive substrate analogs. Previous studies showed that SULTs may catalyze a sequential transfer reaction with the formation of a ternary complex between the enzyme, PAPS and an acceptor substrate, i.e., a Michaelis complex [24,25]. The sulfonation reaction has been proposed to involve an S_N2-like in-line displacement mechanism through a nucleophilic attack on the PAPS sulfonate by the phenoxide of the substrate [14]. Three residues (Lys48, Lys106, and His108) have been proposed to be important for catalysis [15]. The Lys48 may serve to donate its proton to the bridging oxygen as a catalytic acid and stabilize the transition state by interacting with the SO_3 moiety that is being transferred. The Lys106 may function in substrate positioning and in stabilization of the transition state. The His108 may serve as a catalytic base that removes the proton from the acceptor phenolic hydroxyl group and stabilize the transition state by interacting with the SO_3 moiety [15].

In the Michaelis complex (Fig. 3) detected in the present study, the side chain nitrogen of Lys48 was coordinated to one oxygen (3.1 Å) of the SO_3 moiety as well as with the bridging oxygen (2.8 Å). The side chain nitrogen of Lys106 was in a position to form interaction with another oxygen (3.3 Å) of the SO_3 moiety and the acceptor phenolic hydroxyl group (2.9 Å) of the *p*NP[1] molecule. Similarly, the side chain nitrogen (Nε2) of His108 was coordinated with another oxygen (3.2 Å) of the SO_3 moiety and the acceptor phenolic hydroxyl group (2.5 Å). The sulfur atom was found to be located 3.1 Å from the acceptor phenolic hydroxyl group of the *p*NP[1] molecule, and the S–O bond distance of PAPS was determined to be 1.6 Å. The bridging oxygen, the sulfur atom, and the acceptor phenolic hydroxyl group lay approximately in a straight line. The

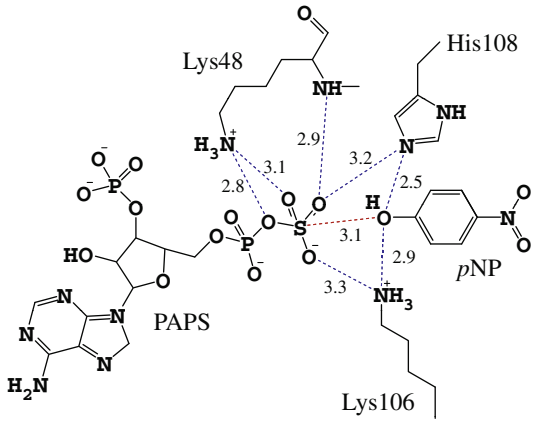

Fig. 3. Schematic representation of the key residues and their coordination in the active site. All possible backbone and side chain coordination of Lys48, Lys106, and His108 in the mSULT1D1–PAPS–*p*NP complex are shown, and their distances are indicated (Å).

angle formed by these three atoms (O–S–O) was 166°. The hydroxyl group of *p*NP was in a proper position for in-line nucleophilic attack. These observations of the Michaelis complex structure strongly support the proposal of a S_N2-like in-line displacement mechanism of the reaction catalyzed by members of the SULT family and are fully consistent with previously reported structural and functional studies [12–18].

In summary, we reported in this paper the structures of four distinct mSULT1D1 crystals prepared using co-crystallization and soaking method. The crystal structures determined were those of mSULT1D1 complexed with PAPS alone, PAPS plus *p*NPS, PAPS plus *p*NP, or PAP plus *p*NP. These structures revealed that mSULT1D1 may catalyze both forward and reverse reactions in respective crystals, with the mSULT1D1–PAPS–*p*NP structure being that of the native Michaelis complex. The data concerning the Michaelis complex reported here strongly supports that the sulfuryl transfer reaction proceeds through an S_N2-like in-line displacement mechanism. The structure of the Michaelis complex is of great importance in understanding precise details required for QM type calculation. Further structural studies on similar Michaelis complexes are warranted in order to understand the mechanism of catalysis of other members of the SULT family.

Acknowledgments

We thank Drs. K. Hasegawa and H. Sakai of the Japan Synchrotron Radiation Research Institute (JASRI) for the kind assistance with data collection using the synchrotron radiation of BL38B1, SPring-8. Synchrotron radiation experiments were carried out with JASRI approval.

This research was supported by the Grant-in-Aid for Scientific Research and the National Project on Protein Structural and Functional Analyses from the Ministry of Education, Culture, Sports, Science and Technology, Japan.

Appendix A. Supplementary data

Supplementary data associated with this article can be found, in the online version, at doi:10.1016/j.bbrc.2009.03.146.

References

[1] R.L. Blanchard, R.R. Freimuth, J. Buck, R.M. Weinshilboum, M.W. Coughtrie, A proposed nomenclature system for the cytosolic sulfotransferase (SULT) superfamily, Pharmacogenetics 14 (2004) 199–211.
[2] H. Zhang, O. Varlamova, F.M. Vargas, C.N. Falany, T.S. Leyh, Sulfuryl transfer: the catalytic mechanism of human estrogen sulfotransferase, J. Biol. Chem. 273 (1998) 10888–10892.
[3] C.N. Falany, Enzymology of human cytosolic sulfotransferases, FASEB J. 11 (1997) 206–216.
[4] M.W. Coughtrie, S. Sharp, K. Maxwell, N.P. Innes, Biology, function of the reversible sulfation pathway catalysed by human sulfotransferases, sulfatases, Chem. Biol. Interact. 109 (1998) 3–27.
[5] Y. Wang, M.R. Spitz, A.M. Tsou, K. Zhang, N. Makan, X. Wu, Sulfotransferase (SULT) 1A1 polymorphism as a predisposition factor for lung cancer: a case-control analysis, Lung Cancer 35 (2002) 137–142.
[6] D.E. Bamber, A.A. Fryer, R.C. Strange, J.B. Elder, M. Deakin, R. Rajagopal, A. Fawole, R.A. Gilissen, F.C. Campbell, M.W. Coughtrie, Phenol sulphotransferase SULT1A1 1 genotype is associated with reduced risk of colorectal cancer, Pharmacogenetics 11 (2001) 679–685.
[7] M. Shimada, R. Terazawa, Y. Kamiyama, W. Honma, K. Nagata, Y. Yamazoe, Unique properties of a renal sulfotransferase, St1d1, in dopamine metabolism, J. Pharmacol. Exp. Ther. 310 (2004) 808–814.
[8] Y. Sakakibara, K. Yanagisawa, Y. Takami, T. Nakayama, M. Suiko, M.C. Liu, Molecular cloning expression and functional characterization of novel mouse sulfotransferases, Biochem. Biophys. Res. Commun. 247 (1998) 681–686.
[9] T. Teramoto, Y. Sakakibara, K. Inada, K. Kurogi, M.C. Liu, M. Suiko, M. Kimura, Y. Kakuta, Crystal structure of MSULT1D1, a mouse catecholamine sulfotransferase, FEBS Lett. 582 (2008) 3909–3914.
[10] T. Teramoto, Y. Sakakibara, M.C. Liu, M. Suiko, M. Kimura, Y. Kakuta, Structural basis for the broad range substrate specificity of a novel mouse cytosolic sulfotransferase—mSULT1D1, Biochem. Biophys. Res. Commun. 379 (2009) 76–80.
[11] A. Allali-Hassani, P.W. Pan, L. Dombrovski, R. Najmanovich, W. Tempel, A. Dong, P. Loppnau, F. Martin, J. Thornton, A.M. Edwards, A. Bochkarev, A.N. Plotnikov, M. Vedadi, C.H. Arrowsmith, Structural and chemical profiling of the human cytosolic sulfotransferases, PLoS Biol. 5 (2007) e97.
[12] M. Negishi, L.G. Pedersen, E. Petrotchenko, S. Shevtsov, A. Gorokhov, Y. Kakuta, L.C. Pedersen, Structure and function of sulfotransferases, Arch. Biochem. Biophys. 390 (2001) 149–157.
[13] E. Chapman, M.D. Best, S.R. Hanson, C.H. Wong, Sulfotransferases: structure, mechanism, biological activity, inhibition, and synthetic utility, Angew. Chem. Int. Ed. Engl. 43 (2004) 3526–3548.
[14] Y. Kakuta, L.G. Pedersen, C.W. Carter, M. Negishi, L.C. Pedersen, Crystal structure of estrogen sulphotransferase, Nat. Struct. Biol. 4 (1997) 904–908.
[15] Y. Kakuta, E.V. Petrotchenko, L.C. Pedersen, M. Negishi, The sulfuryl transfer mechanism. Crystal structure of a vanadate complex of estrogen sulfotransferase and mutational analysis, J. Biol. Chem. 273 (1998) 27325–27330.
[16] L.C. Pedersen, E. Petrotchenko, S. Shevtsov, M. Negishi, Crystal structure of the human estrogen sulfotransferase–PAPS complex: evidence for catalytic role of Ser137 in the sulfuryl transfer reaction, J. Biol. Chem. 277 (2002) 17928–17932.
[17] R.H. Hoff, P.G. Czyryca, M. Sun, T.S. Leyh, A.C. Hengge, Transition state of the sulfuryl transfer reaction of estrogen sulfotransferase, J. Biol. Chem. 281 (2006) 30645–30649.
[18] P. Lin, W. Yang, L.C. Pedersen, M. Negishi, L.G. Pedersen, Searching for the minimum energy path in the sulfuryl transfer reaction catalyzed by human estrogen sulfotransferase: role of enzyme dynamics, Int. J. Quantum Chem. 106 (2006) 2981–2998.
[19] Z. Otwinowski, W. Minor, Processing of X-ray diffraction data collected in oscillation mode, Methods Enzymol. 276 (1997) 307–326.
[20] A. Vagin, A. Teplyakov, An approach to multi-copy search in molecular replacement, Acta Crystallogr. D Biol. Crystallogr. 56 (2000) 1622–1624.
[21] G.N. Murshudov, A.A. Vagin, E.J. Dodson, Refinement of macromolecular structures by the maximum-likelihood method, Acta Crystallogr. D Biol. Crystallogr. 53 (1997) 240–255.
[22] P. Emsley, K. Cowtan, Coot: model-building tools for molecular graphics, Acta Crystallogr. D Biol. Crystallogr. 60 (2004) 2126–2132.
[23] A.A. Vaguine, J. Richelle, S.J. Wodak, SFCHECK: a unified set of procedures for evaluating the quality of macromolecular structure-factor data and their agreement with the atomic model, Acta Crystallogr. D Biol. Crystallogr. 55 (1999) 191–205.
[24] T.S. Leyh, The physical biochemistry and molecular genetics of sulfate activation, Crit. Rev. Biochem. Mol. Biol. 28 (1993) 515–542.
[25] E. Tyapochkin, P.F. Cook, G. Chen, Isotope exchange at equilibrium indicates a steady state ordered kinetic mechanism for human sulfotransferase, Biochemistry 47 (2008) 11894–11899.